ACS APPLIED MATERIALS & INTERFACES

Research Article

www.acsami.org

Effects of Solution Temperature on Solution-Processed High-Performance Metal Oxide Thin-Film Transistors

Keun Ho Lee,[†] Jee Ho Park,[†] Young Bum Yoo,[†] Woo Soon Jang,[†] Jin Young Oh,[†] Soo Sang Chae,[†] Kyeong Ju Moon,[‡] Jae Min Myoung,[‡] and Hong Koo Baik*,[†]

[†]Display and Plasma Research Lab, Department of Materials Science and Engineering, Yonsei University, 134 Shinchong-dong, Seoul 120-750, Republic of Korea

[‡]Information and Electronic Materials Research Lab, Department of Materials Science and Engineering, Yonsei University, 134 Shinchong-dong, Seoul 120-750, Republic of Korea

Supporting Information

ABSTRACT: Herein, we report a novel and easy strategy for fabricating solution-processed metal oxide thin-film transistors by controlling the dielectric constant of H_2O through manipulation of the metal precursor solution temperature. As a result, indium zinc oxide (IZO) thin-film transistors (TFTs) fabricated from IZO solution at 4 °C can be operated after annealing at low temperatures (~250 °C). In contrast, IZO TFTs fabricated from IZO solutions at 25 and 60 °C must be annealed at 275 and 300 °C, respectively. We also found that IZO TFTs fabricated from the IZO precursor solution at 4 °C had the highest mobility of 12.65 $cm^2/(V\ s)$, whereas the IZO TFTs fabricated from IZO precursor solutions at 25 and 60 °C had field-effect mobility of 5.39 and 4.51 $cm^2/(V\ s)$, respectively, after annealing at 350 °C. When the IZO precursor solution is at 4 °C, metal cations such as indium (In^{3+}) and zinc ions (Zn^{2+}) can be fully surrounded by H_2O molecules, because of the higher dielectric constant of H_2O at lower temperatures. These chemical complexes in the IZO precursor solution at 4 °C are advantageous for thermal hydrolysis and condensation reactions yielding a metal oxide lattice, because of their high potential energies. The IZO TFTs fabricated from the IZO precursor solution at 4 °C had the highest mobility because of the formation of many metal−oxygen−metal (M-O-M) bonds under these conditions. In these bonds, the ns-orbitals of the metal cations overlap each other and form electron conduction pathways. Thus, the formation of a high proportion of M-O-M bonds in the IZO thin films is advantageous for electron conduction, because oxide lattices allow electrons to travel easily through the IZO.

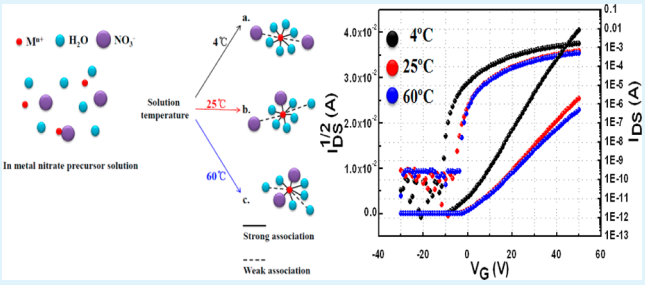

KEYWORDS: *solution-processed, effects of solution temperature, metal oxide thin film transistors, dielectric constant, ion pairing, solvation*

1. INTRODUCTION

To date, thin-film transistors (TFTs) based on solution-processed amorphous oxide semiconductors (AOSs), such as amorphous indium zinc oxide (IZO), zinc tin oxide (ZTO), indium gallium oxide (IGO), and indium gallium zinc oxide (IGZO), have been investigated.[1−4] However, solution-processed AOS-TFTs have suffered from low mobility, compared to vacuum-processed AOS-TFTs. Recently, several groups have reported efficient methods for enhancing the field-effect mobility and lowering the metal oxide film annealing temperature. Jeong et al.[4] reported that gallium doping lowers the processing temperature because Ga atoms can induce a metal−oxygen lattice that forms an electron pathway. Banger et al.[5] reported on the formation of IZO films using a "sol gel on chip" process. In this process, highly reactive metal alkoxide precursors are used, so that a hydrolysis reaction occurs directly on the surface of the IZO film. Kim et al.[6] deposited solution-processed IZO thin films using combustion chemistry. The advantage of this technique is the generation of high local temperatures, which can convert the precursors to metal oxides. These processes have produced amorphous oxide TFTs with high mobility after annealing at temperatures under <300 °C.

To address this mobility issue, we have employed a solution chemistry called ion pairing[7−13] in order to fabricate solution-processed TFTs. In particular, we focused on changing the dielectric constant of molecules such as 2-methoxyethanol (2ME) and H_2O so that solution chemistry could be used effectively. The term "ion pairing" refers to the association of oppositely charged ions in the electrolyte solutions to form distinct chemical species called ion pairs. These ion pairs can be classified as solvent-shared ion pairs (SIPs) and contact ion pairs (CIPs). In this solution chemistry process, two distinct

Received: December 27, 2012
Accepted: March 5, 2013
Published: March 5, 2013

   dx.doi.org/10.1021/am3032629 | ACS Appl. Mater. Interfaces 2013, 5, 2585−2592

chemical species can be formed by changing the dielectric constant of the dissociating medium such as the H_2O or alcohol. Generally, the dielectric constant increases as the temperature of the dissociating medium decreases.[14,15] When the dissociating medium has a high dielectric constant, SIPs are predominantly formed, and vice versa.

In this study, to reduce the processing temperature and enhance the field-effect mobility, we have developed a novel and easy strategy for fabricating solution-processed metal oxide TFTs by controlling the dielectric constant of H_2O and 2ME through manipulation of the solution temperatures. We have tried to synthesize dissolved metal salts at various solution temperatures. Metal cations that have fully solvated with H_2O molecules (SIPs) have higher potential energies for the thermally driven hydrolysis and condensation reactions than do metal cations with partial solvation shells and strong associations with anions (CIPs). Therefore, IZO thin films exhibit a high percentage of oxide lattices (as opposed to lattices with oxide vacancies or hydroxides) when there are fully solvated metal cations in the precursor solution. This high percentage of oxide lattices is advantageous for electron conduction, because oxide lattices allow electrons to travel through the metal oxides. As a result, IZO TFTs fabricated from an IZO solution at 4 °C can be operated after annealing at low temperatures (~250 °C). In contrast, IZO TFTs fabricated from IZO solutions at 25 and 60 °C must be annealed at 275 and 300 °C, respectively. We also find that the IZO TFTs fabricated from IZO solutions at 4 °C have the highest mobility of 12.65 $cm^2/(V\ s)$, whereas IZO TFTs fabricated from IZO solutions at 25 and 60 °C have field-effect mobility of 5.39 and 4.51 $cm^2/(V\ s)$, respectively, when annealed at 350 °C.

2. EXPERIMENTAL SECTION

2.1. Precursor Solution Preparation. All reagents were purchased from Sigma–Aldrich Chemicals and were used without further purification. The precursor solution for the IZO thin film was synthesized by dissolving the metal salt precursor in solvents maintained at various temperatures (4, 10, 15, 20, 25, and 60 °C) using a chiller. Then, 0.1 M zinc nitrate hexahydrate [$Zn(NO_3)_2{\cdot}6H_2O$] and 0.1 M indium nitrate hydrate [$In(NO_3)_3{\cdot}xH_2O$] were separately dissolved in 2-methoxyethanol at the intended solution temperature maintained using a chiller. These two stock solutions were then mixed and stirred for 12 h at various temperatures (see Figure S1 in the Supporting Information).

2.2. Film Deposition and Thin-Film Transistor Fabrication. Before the IZO thin film deposition, the substrates were cleaned with a piranha cleaning solution (3:1 H_2SO_4/H_2O_2) for 1 h and rinsed with deionized water. For the deposition of the IZO thin film from the IZO solutions at various temperatures, the IZO solution was first filtered through a 0.2-μm polymer membrane syringe filter. Then, the IZO solution was spin-coated on a 200 nm-thick SiO_2/P + Si substrate at 4000 rpm for 30 s. The deposited IZO thin film was annealed at 350 °C for 2 h on a hot plate in air. To fabricate an IZO TFT, an Al source and drain electrodes with thicknesses of 100 nm were evaporated through a metal shadow mask (~10^{-6} Torr). The channel length and width were 150 and 1000 μm, respectively. The current–voltage characteristics of all the fabricated transistors were measured in darkness in ambient air using an Agilent 4145B semiconductor parameter analyzer.

2.3. Solution and Film Characterization. Raman spectroscopy (Horiba Jobin–Yvon/LabRam HR) was performed to investigate the ionic behaviors in the IZO solution. The main difficulty in the Raman spectroscopic investigations conducted at different solution temperatures was in the design of a container that could maintain the solution temperature (4, 25, or 60 °C). Briefly, the IZO solution samples were excited with the 514.5-nm line of an Ar-ion laser at a power level of 1 mW to obtain their Raman spectra. Depolarized spectra were accumulated for exposure periods of 60 s.

The chemical and electronic structures of the IZO thin films were examined by performing X-ray photoelectron spectroscopy (XPS; Thermo VG, U.K.). The surface XPS data were collected using monochromatic Al Kα radiation (1486.6 eV) in an ultrahigh-vacuum system with a base pressure of -10^{-10} mbar. The binding energy shift was corrected using the C 1s peak (284.8 eV). The XPS data for the metal oxide films were obtained after the samples were sputter cleaned via Ar-ion etching.

3. RESULTS AND DISCUSSION

The $Zn(NO_3)_2{\cdot}6H_2O$ and $In(NO_3)_3{\cdot}xH_2O$ ionize in a dissociating medium such as 2ME. Consequently, the metal cation undergoes a solvation reaction and becomes surrounded by 2ME/H_2O molecules. The Zn^{2+} ion has a solvation number of 6 and forms an octahedral inner coordination shell.[5] The In^{3+} ion has a solvation number of 5–6.[10] The solvation number indicates the number of H_2O molecules associated with the metal cation.[16,17] The 2ME solution containing H_2O has metal cation coordination in which the H_2O also participates in the solvate.[18] The driving force for the formation of the solvation shell around the metal cation is the dielectric constant of the solvent. Therefore, the dielectric constant makes the solvent a dissociating medium by decreasing the electrostatic forces between the cations and anions.[19]

In the deposition of solution-processed metal oxide thin films, the structures of the solvated metal cations are important for the thermally driven hydrolysis and condensation reactions. The thermally driven hydrolysis reaction involves the removal of the NO_3^- ion bonded to the Zn^{2+} ion by H_2O molecules originating from the $Zn(NO_3)_2{\cdot}6H_2O$ itself.[18] Metal cations that are fully surrounded by the H_2O molecules can have high potential energies for these thermally driven hydrolysis and condensation reactions yielding metal oxide lattices. In contrast, metal cations that are surrounded by H_2O molecules and anions will need more thermal energy to form metal oxide lattices, because anions such as NO_3^- disrupt these hydrolysis and condensation reactions.[20] Therefore, to promote the thermally driven hydrolysis reactions, it is more advantageous to form metal cations fully solvated with H_2O molecules instead of metal cations with partial solvation shells and partially bonded to anions. For this reason, we focused on metal cations solvated with H_2O molecules instead of 2ME/H_2O molecules, because H_2O molecules have a higher dielectric constant (ε_r = 78.5) than 2ME molecules (ε_r = 17.2) at room temperature.[14,15] To obtain a high dielectric constant of H_2O, we synthesized dissolved $Zn(NO_3)_2{\cdot}6H_2O$ and $In(NO_3)_3{\cdot}xH_2O$ at a solution temperature of 4 °C (Figure 1a). Typically, the dielectric constant increases as the temperature decreases. At room temperature, In^{3+} and Zn^{2+} ions could be solvated with NO_3^- and H_2O molecules (Figure 1b). When the solution temperature is increased to 60 °C, more NO_3^- could be attached to the metal cations (Figure 1c). Thus, at these temperatures, the metal cations are not fully surrounded by H_2O molecules. NO_3^- is bonded to the metal cations in solution because the dielectric constant of the H_2O molecules has decreased.[8] On the other hand, the metal cations were mainly solvated with H_2O molecules below room temperature, and In^{3+} and Zn^{2+} ions are likely fully surrounded by H_2O molecules, because of their higher dielectric constant (ε_r = 86.4 at ~4 °C).[15] Therefore, we can change the dielectric constant of the H_2O molecules by controlling the solution temperature

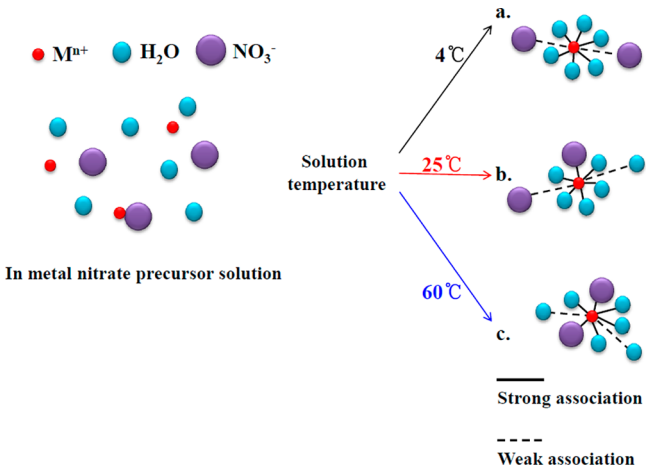

Figure 1. Schematic illustration of ionic behaviors in metal nitrate precursor solutions with different temperatures.

to enhance the thermally driven hydrolysis and condensation reactions.

Hereafter, for the sake of simplicity, the IZO solutions at 4, 25, and 60 °C are denoted as 4S, 25S, and 60S, respectively.

We first investigated the 4S, 25S, and 60S by performing Raman spectroscopy. Several studies have provided evidence that the degree of solvation of metal cations is dependent on the solvent temperature.[8,10−13] The Raman spectra were measured for 1 M 4S, 25S, and 60S. The obtained Raman spectra were fitted well by three components, indicating that the NO_3^- species formed at least three different ionic structures, as shown in Figure 2. This figure shows the three NO stretching bands in the Raman spectra centered at 1025, 1045, and 1060 cm^{-1}. According to previous studies,[8,21] the lower, middle, and high Raman shifts correspond to NO_3^- partially associated with metal cations, NO_3^- weakly associated with metal cations, and NO_3^- strongly associated with metal cations, respectively. Figure 2d shows the quantitative analysis of each frequency component for the 4S, 25S, and 60S. It is found that metal cations fully solvated with H_2O molecules could be formed when the solution temperature was decreased (see Figure 1).

We also investigated the difference in the structural evolution of the IZO thin films deposited from 4S, 25S, and 60S. The IZO thin films were analyzed by performing X-ray photoelectron spectroscopy (XPS). Figure 3 shows the O 1s XPS spectra for the IZO thin films. The peaks centered at ~529.9 and 531.4 eV can be assigned to the oxygen in the oxide lattices without oxygen vacancies and with oxygen vacancies, respectively. The feature at 532.4 eV can be assigned to the oxygen in the hydroxide.[22] Note that the IZO thin film deposited from 4S is composed of a high quantity of oxide lattices in Figure 3a. These metal oxide lattices were formed to a greater extent by the thermally driven hydrolysis and condensation reactions of the metal cations highly solvated with H_2O molecules. In contrast, the IZO thin films deposited from 25S and 60S had a low quantity of oxide lattices and a high amount of lattices that had oxygen vacancies and hydroxides, as shown in Figures 3b and 3c. In particular, as shown in Figure 3d, the oxide lattice content of the IZO thin

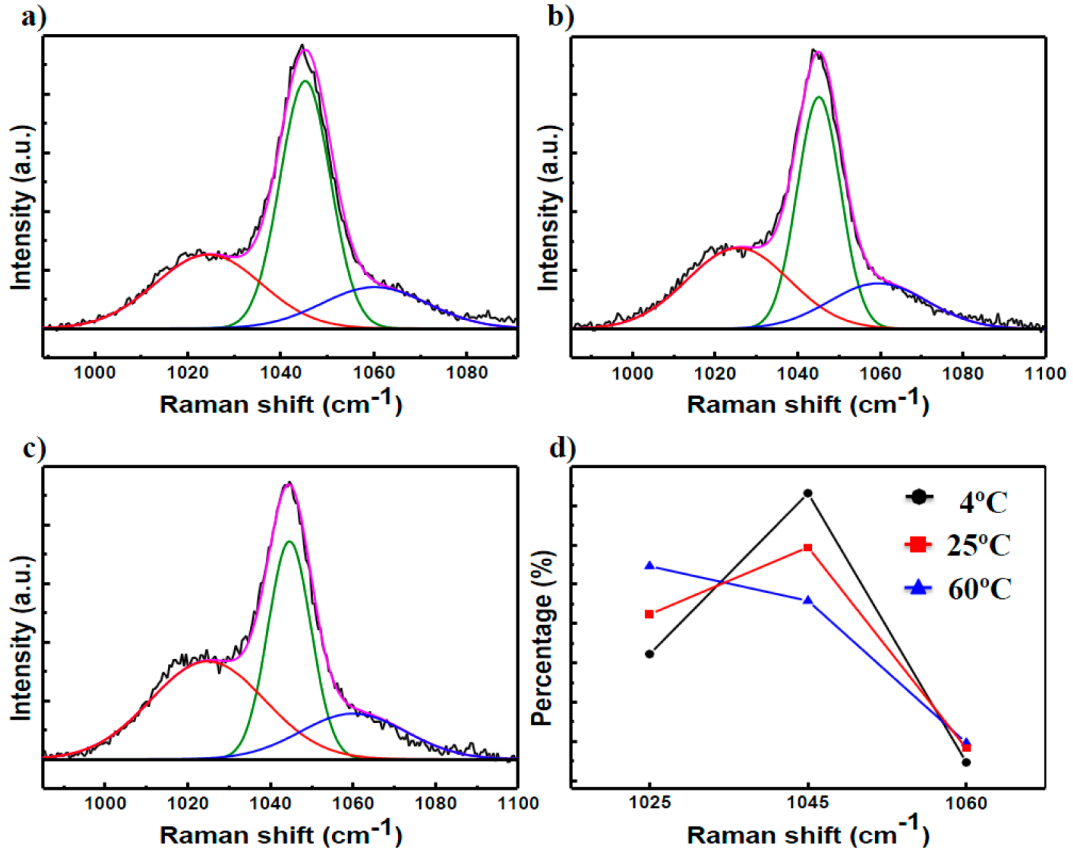

Figure 2. Raman spectra of (a) 4S, (b) 25S, and (c) 60S. (d) The percentage of each component for 4S, 25S, and 60S was calculated based on the area integration of each peak.

dx.doi.org/10.1021/am3032629 | ACS Appl. Mater. Interfaces 2013, 5, 2585−2592

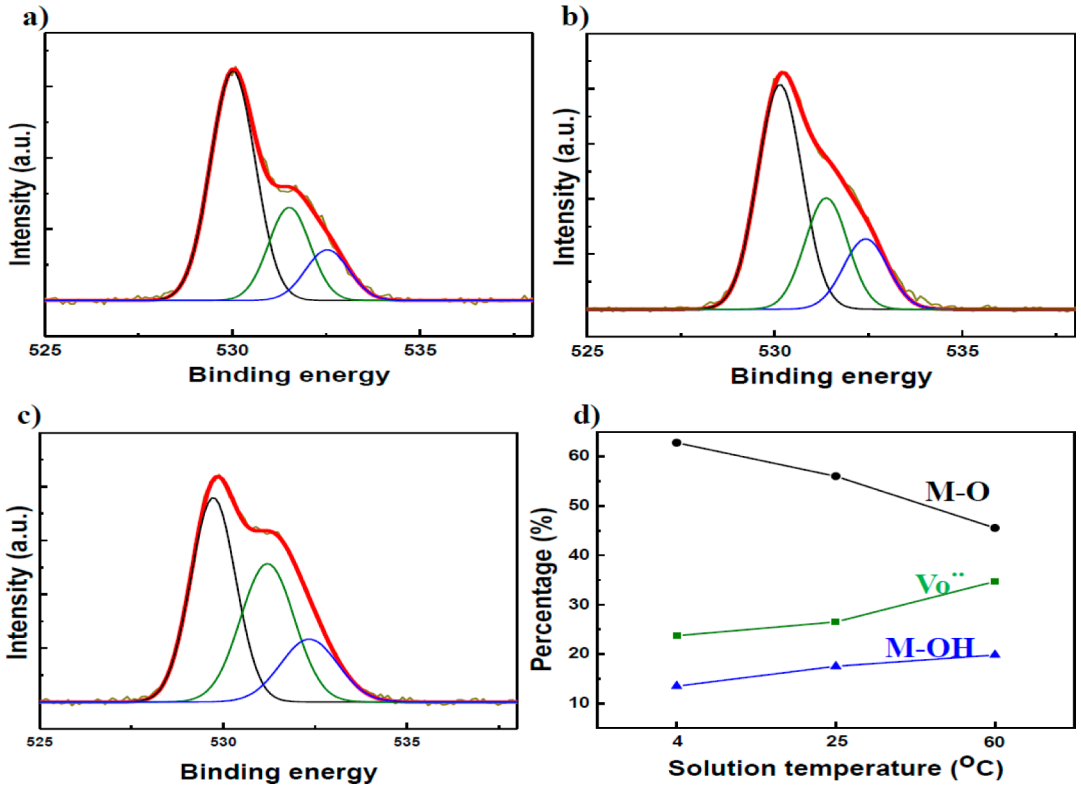

Figure 3. O 1s XPS spectra for the IZO thin films annealed at 350 °C deposited from (a) 4S, (b) 25S, and (c) 60S. (d) The percentage of oxide lattices, lattices with oxygen vacancies, and oxygen in hydroxide. The percentages were calculated based on the area integration of each O 1s peak.

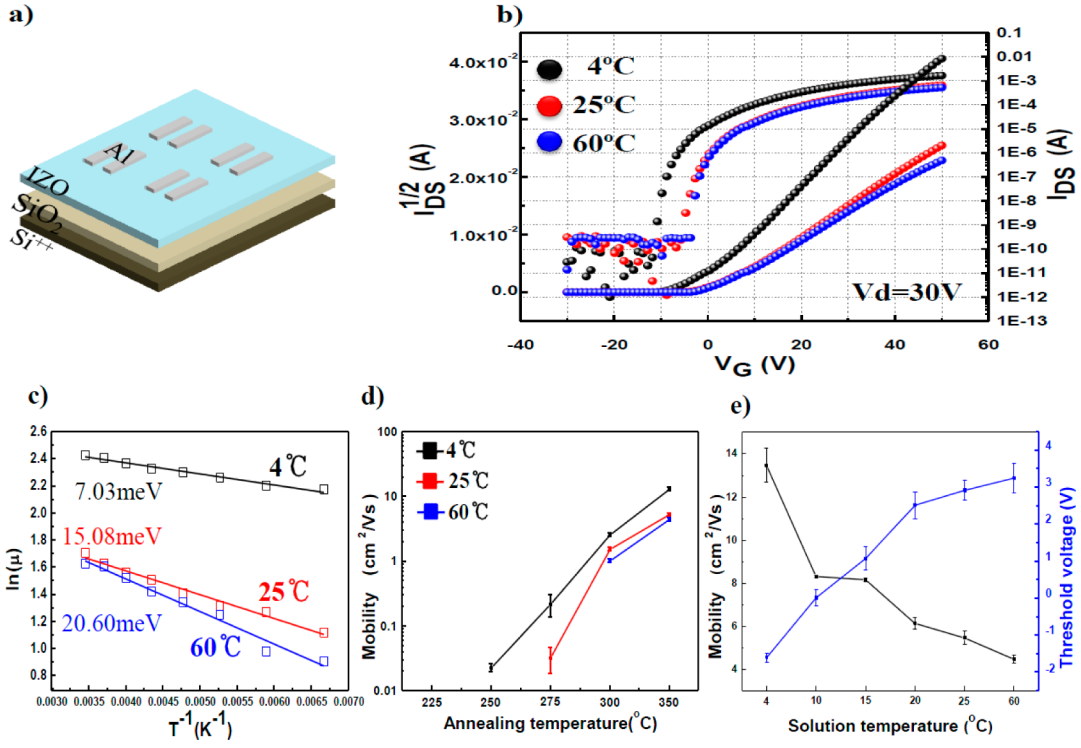

Figure 4. (a) Schematic illustration of the TFT structure used in this study. (b) Transfer characteristics of IZO TFTs deposited at the indicated solution temperatures. (c) Plots of ln μ vs T^{-1} for IZO TFTs deposited at the indicated solution temperatures. (d) Dependence of the field-effect mobility on annealing temperature as plotted on a log scale with error bars for IZO TFTs deposited at the indicated solution temperatures. (e) Dependence of the field-effect mobility and threshold voltage (V_{th}) on the solution temperature from 4 to 60 °C for IZO TFTs annealed at 350 °C.

films increased from 45.5% to 63.8% as the precursor solution temperature decreased. Since the metal cations are highly solvated with H_2O molecules at low temperatures, they have higher potential energies for the hydrolysis and condensation

dx.doi.org/10.1021/am3032629 | ACS Appl. Mater. Interfaces 2013, 5, 2585−2592

reactions than do the metal cations only partially solvated with H_2O molecules.

An electrical investigation of the IZO thin films was carried out using the bottom gate TFT structure described in Figure 4a. The performance of the IZO TFTs deposited at different solution temperature was assessed through analysis of their field-effect mobility, threshold voltage, and thermal activation energy for carrier transport.

Figure 4b shows the transfer curve of the IZO TFTs fabricated from the 4S, 25S, and 60S. Interestingly, it can be observed that IZO TFT fabricated from 4S has the highest on-current and field-effect mobility at 30 V_{DS}. Details of the electrical performance, as a function of the solution temperature, are summarized in Figure 4e. The field-effect mobility of the IZO TFTs decreased from 12.65 to 4.09 $cm^2/(V\ s)$ as the solution temperature increased from 4 °C to 60 °C. The TFT performance parameters, including the field-effect mobility (μ), threshold voltage (V_{th}), and on-to-off current ratio (I_{on}/I_{off}), are summarized in Table 1. Together, these results show that the decrease in solution temperature improves the electron transport through the IZO. As mentioned above, the IZO thin film deposited from 4S has the highest quantity of oxide lattices (see Figure 3). This large proportion of oxide lattices indicates the formation of many metal−oxygen−metal (M-O-M) bonds. In metal oxide thin films, the electron conduction mechanism is related to the M-O-M bonds. Hosono et al. suggested that the conduction band minimum in metal oxide semiconductors consists of metal cation ns-orbitals.[23] These ns-orbitals of the metal cations overlap each other to form electron conduction pathways.[24] Thus, the degree to which oxide lattices form significantly affects the electrical properties of oxide-based transistors, and it is advantageous for electron conduction to form a high proportion of M-O-M bonds in the IZO thin films, because the oxide lattices allow electrons to travel through the IZO. In addition, the number of oxygen vacancies can be reduced by decreasing the solution temperature. Filling of the oxygen vacancies has been reported to improve the TFT mobility, since vacancies can act as scattering centers.[25]

Table 1. Electrical Performance of Solution-Processed Metal Oxide TFTs Annealed at 350 °C

solution temperature [°C]	field-effect mobility, μ [$cm^2/(V\ s)$]	threshold voltage, V_{th} [V]	on/off current ratio, I_{on}/I_{off}
	IZO		
4	12.65	−1.61	$>10^7$
25	5.39	2.83	$\sim10^7$
60	4.51	2.91	$\sim10^6$
	GIO		
4	5.67	4.55	$>10^7$
25	2.57	5.24	$\sim10^6$
	GIZO		
4	2.69	1.45	$\sim10^7$
25	0.51	5.21	$\sim10^6$
	ZTO		
4	2.18	−0.57	$\sim10^7$
25	0.98	3.90	$\sim10^6$

To further investigate the changes in field-effect mobility, relative to solution temperature, the thermal activation energies for carrier transport in IZO TFTs fabricated from 4S, 25S, and 60S were evaluated from the slope of the ln μ vs T^{-1} plots within a temperature range of 150−290 K, as shown in Figure 4c, and from the slope of the mobility vs V_g-V_{on} plots at temperatures of 150, 230, and 290 K, as shown in Figure S6 in the Supporting Information. All of the IZO thin films were annealed at 350 °C for 2 h. Measurement of the temperature-dependent field-effect mobility was performed in a vacuum chamber with a cryogenic probe station (Lake Shore/TTPX). A decreasing trend for E_a indicates that, as the gate voltage increases, the energy difference between the filled trap states and the transport states decreases as a result of shifts in the Fermi level toward the mobility edge.[26] In our experiment, the lowest E_a value was observed for the IZO TFT fabricated from 4S (E_a = 7.03 meV), whereas the IZO TFTs fabricated from 25S and 60S had E_a values of 15.08 and 20.60 meV, respectively. A low E_a value indicates that the energy difference between the filled trap states and the transport states is small. This means that a low amount of energy is needed for bandlike transport.

We also analyzed the effects of the solution temperature on the performance of the IZO TFT. Figure 4d shows plots of the field-effect mobility versus annealing temperature between 225 °C and 350 °C for the IZO TFTs fabricated at different solution temperatures. The electrical performance of the TFTs is also highly dependent on the annealing temperature. Regardless of the solution temperature, the field-effect mobility decreased as the annealing temperature decreased, since the Zn−Zn and In−In interaction distances are greater for low annealing temperatures, which generates shallow localized states beneath the conduction band minima and, in turn, decreases the carrier mobility.[27] The field-effect mobility of the IZO TFTs fabricated from 4S, 25S, and 60S were different for certain annealing temperatures. The IZO TFTs were all inactive when annealed at 225 °C, since this annealing temperature is inadequate for the removal of solvent molecules, anion molecules, and other impurities, and for the formation of metal oxide lattices. Similar results have been obtained in several studies.[28,29] The IZO TFT fabricated from 4S became active when it was annealed at 250 °C, and its the field-effect mobility was further dramatically enhanced from 0.02 to 12.65 $cm^2/(V\ s)$ when the annealing temperature was increased from 250 and 350 °C. The IZO TFT fabricated from 25S was active when it was annealed at 275 °C, and its field-effect mobility was enhanced from 0.03 $cm^2/(V\ s)$ to 5.39 $cm^2/(V\ s)$ when the annealing temperature was increased from 275 °C to 350 °C. The IZO TFT fabricated from 60S was active when it was annealed 300 °C, which is the highest activating annealing temperature found in this study. The field-effect mobility of the IZO TFT fabricated from 60S was slightly enhanced from 1.02 $cm^2/(V\ s)$ to 4.51 $cm^2/(V\ s)$ when the annealing temperature was increased from 300 °C to 350 °C.

We believe that the differences in the appropriate annealing temperatures are due to the structure of the solvated metal cations in the precursor solutions prepared at various temperatures (see Figure 1). In the 4S, the metal cations are mainly surrounded by H_2O molecules, and this structure of solvated metal cations has a high potential energy for the thermally driven hydrolysis and condensation reactions. Thus, oxide lattices, which play important roles in transporting electrons, are formed at the lowest annealing temperature (~250 °C). On the other hand, at higher temperatures, metal cations are partially surrounded by NO_3^-, which hinders the thermally driven hydrolysis and condensation reactions. Since the structures of the solvated metal cations in solution are different at these temperatures, the oxide lattices in the IZO

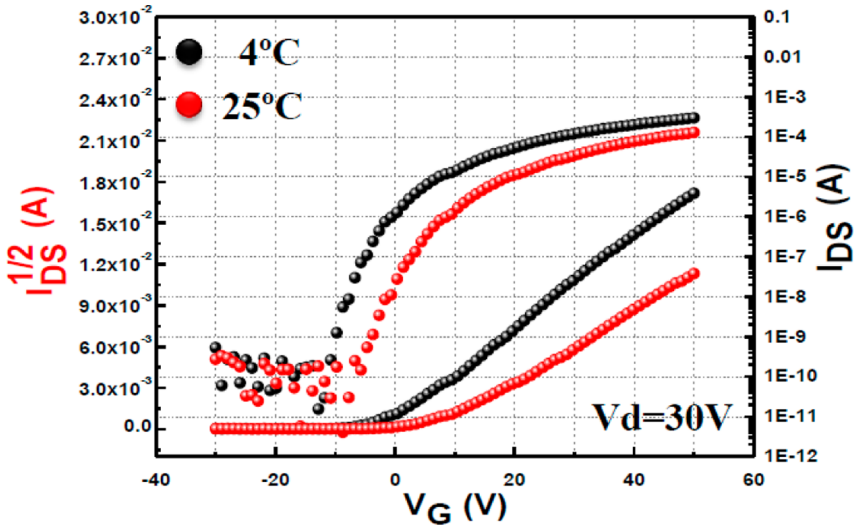

Figure 5. Transfer characteristics of ZTO TFTs deposited at the indicated solution temperatures. ZTO thin films were annealed at 350 °C.

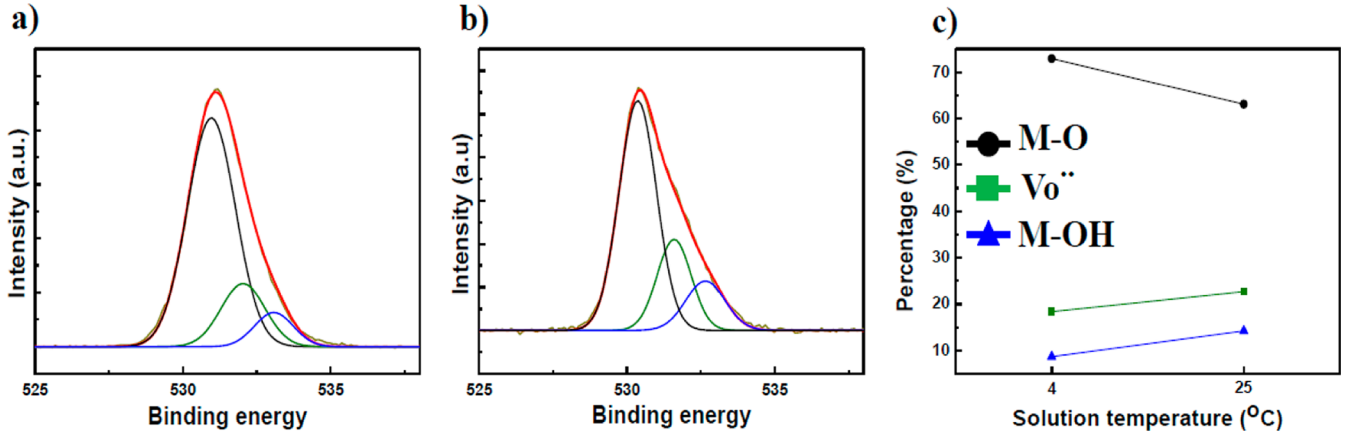

Figure 6. O 1s XPS spectra for the ZTO thin films annealed at 350 °C deposited from (a) 4S and (b) 25S. (c) Percentages of the oxide lattices, lattice with oxygen vacancies, and oxygen in hydroxide. The percentages were calculated based on the area integration of each O 1s peak. The colored lines indicate the peaks that are from the oxide lattices without oxygen vacancies (~530.5 eV), the oxide lattices with oxygen vacancies (~531.9 eV), and the hydroxide (~532.6 eV).[34]

films fabricated from 25S and 60S are formed at 275 and 300 °C, respectively. Therefore, the structures of the solvated ions affect the electrical performance. In particular, in this study, we provide evidence that the design of the ionic structures in solution is important for the formation of oxide lattices at low annealing temperatures, which is necessary for achieving high electrical performance in metal oxide TFTs.

Figure 4e shows that the threshold voltage of the IZO TFTs increased from −1.61 V to 2.91 V as the solution temperature increased from 4 °C to 60 °C. This variation in the threshold voltage can be explained by the results of the O 1s XPS analysis. The IZO thin film deposited from 4S had fewer hydroxides and fewer lattice-containing oxygen vacancies than did the IZO thin films deposited at high solution temperatures. Hydroxyl groups are well-known trap sties for electrons,[30,31] and the number of trap sites influences the threshold voltage.[32] When the number of hydroxyl groups decreases, the threshold voltage shifts toward a negative bias, because of the absence of trap sites. Therefore, the threshold voltage of IZO TFTs fabricated from 4S is shifted in a negative direction to −1.61 V, whereas the threshold voltages of the IZO TFTs fabricated from 25S and 60S are shifted in a positive direction to 2.83 and 2.91 V, respectively (see Figure 3).

In short, the IZO TFTs fabricated with 4S had the highest field effect mobility of 12.65 $cm^2/(V\ s)$ and a threshold voltage of −1.61 V, and the thin films fabricated with 25S and 60S had field effect mobilities of 5.39 and 4.51 $cm^2/(V\ s)$, respectively, and threshold voltages of 2.83 and 2.91 V, respectively.

We also investigated whether this process depends on the oxide material. In particular, we examined several oxide materials such as GIO, GIZO, and ZTO. In this experiment, we only tested metal oxide precursor solutions at 4 and 25 °C, since the electrical properties of IZO TFTs fabricated from 25S and 60S, such as the field-effect mobility, had only relatively small differences. The GIO and GIZO were deposited with a metal nitrate precursor solution. The electrical performance of the GIO and GIZO TFTs fabricated at 4 and 25 °C and the XPS structural analysis of the GIO and GIZO thin films are shown in the Supporting Information. The ZTO thin films were deposited with a metal chloride precursor solution. When the ZTO solution temperature is increased, the chlorine (Cl^-) ion behaves like a nitrate (NO_3^-) ion in the metal precursor solution. Figure 5 shows the transfer curves of the ZTO TFTs

fabricated from the ZTO solution at 4 and 25 °C (denoted as 4S and 25S, respectively). The ZTO solution was synthesized from a chloride-based precursor, unlike the IZO, IGO, and IGZO solutions, which were synthesized from a nitrate-based precursor. In the ZTO solution, the Cl^- ions can behave similarly to the NO_3^- ions. Since the electric force between the metal cations and the Cl^- is stronger than the bonding between the metal cations and the solvent molecules, the Cl^- is strongly associated with the metal cations. The resultant solvation shell of the metal cations can be regarded as a complex containing Cl^-.[33] As we noted above, if the metal cation is partially bonded to Cl^-, the Cl^- will prevent the hydrolysis reaction, and more thermal energy will be needed for the hydrolysis and condensation reactions. Therefore, to make the Cl^- weakly associated with the metal cations, we adjusted the solution temperature to below 25 °C to change the dielectric constant of the H_2O molecules. In 4S, the electrostatic force between the metal cations and the Cl^- is weaker than the bonding between the metal cations and the H_2O molecules. The resultant solvation shell of the metal cations can be considered as a complex containing only H_2O molecules and no Cl^-. These distinctively different structures of the solvated metal cations in 4S and 25S cause different quantities of oxide lattices to be formed by the thermally driven hydrolysis and condensation reactions, as shown in Figure 6. The ZTO TFT fabricated from 4S had a high on-current and a high field-effect mobility, because of its large proportion of oxide lattices. When the solution temperature was increased from 4 to 25 °C, the threshold voltage of the ZTO TFTs increased, because the amount of hydroxyl groups increased from 8.7% to 14.2%.

4. CONCLUSIONS

We have reported a novel and easy strategy for fabricating solution-processed metal oxide thin-film transistors (TFTs) by controlling the dielectric constant through manipulation of the solution temperature. We synthesized dissolved metal salts at various solution temperatures to obtain metal cations fully surrounded by solvation shells of H_2O molecules. Ultimately, in the 4S, the metal cations were fully solvated with H_2O molecules, because of the increase in the dielectric constant of the H_2O molecules. However, the metal cations are partially surrounded with NO_3^- at higher solution temperatures, because of a decrease in the dielectric constant of the H_2O molecules. Metal cations fully solvated with H_2O molecules have more potential energy for the thermally driven hydrolysis and condensation reactions than metal cations with only partial H_2O solvation shells. Therefore, indium zinc oxide (IZO) thin films deposited from solutions with fully solvated metal cations have a high percentage of oxide lattices. A high percentage of oxide lattices is advantageous for electron conduction, since the oxide lattices allows the electrons to travel through the IZO. As a result, IZO TFTs fabricated from an IZO solution at 4 °C can be annealed at a low temperature (~250 °C), and the IZO TFTs fabricated from an IZO solution at 4 °C had the highest field-effect mobility of 12.65 $cm^2/(V\ s)$ when annealed at 350 °C.

■ ASSOCIATED CONTENT

Supporting Information

The electrical performance of the GIO and GIZO TFTs fabricated at 4 and 25 °C and XPS structural analyses of the GIO and GIZO thin films are discussed in the Supporting Information. We also describe the experimental procedures for the GIO, GIZO, and ZTO TFTs experiments. This material is available free of charge via the Internet at http://pubs.acs.org.

■ AUTHOR INFORMATION

Corresponding Author

*Tel.: +82-10-9043-2838. E-mail: thinfilm@yonsei.ac.kr.

Notes

The authors declare no competing financial interest.

■ ACKNOWLEDGMENTS

This work was supported by the National Research Foundation of Korea (NRF, No. 2012-0008721) funded by the government of Korea (MEST). Further funding came from LG Display.

■ REFERENCES

(1) Lee, D. H.; Chang, Y. J.; Herman, G. S.; Chang, C. H. *Adv. Mater.* **2007**, *19*, 843−847.
(2) Park, J. H.; Choi, W. J.; Oh, J. Y.; Chae, S. S.; Jang, W. S.; Lee, S. J.; Song, K. M.; Baik, H. K. *Jpn. J. Appl. Phys.* **2011**, *50*, 070201.
(3) Park, J. H.; Choi, W. J.; Chae, S. S.; Oh, J. Y.; Lee, S. J.; Song, K. M.; Baik, H. K. *Jpn. J. Appl. Phys.* **2011**, *50*, 080202.
(4) Jeong, S.; Ha, Y. G.; Moon, J.; Facchetti, A.; Marks, T. J. *Adv. Mater.* **2010**, *22*, 1346−1350.
(5) Banger, K. K.; Yamashita, Y.; Mori, K.; Perterson, R. L.; Leedham, T.; Rickard, J.; Sirringhaus, H. *Nat. Mater.* **2011**, *10*, 45−50.
(6) Kim, M. G.; Kanatzidis, M. G.; Facchetti, A.; Marks, T. J. *Nat. Mater.* **2011**, *10*, 382−388.
(7) Marcus, Y.; Hefter, G. *Chem. Rev.* **2006**, *106*, 4585−4621.
(8) Ikushima, Y.; Saito, N.; Arai, M. *J. Phys. Chem. B* **1998**, *102*, 3029−3035.
(9) Inada, Y.; Hayashi, H.; Sugimoto, K.; Funahashi, S. *J. Phys. Chem. A* **1999**, *103*, 1401−1406.
(10) Irish, D. E.; Jarv, T. *Discuss. Faraday Soc* **1977**, *64*, 95−101.
(11) Bulmer, J. T.; Irish, D. E.; Ödberg, L. *Can. J. Chem.* **1975**, *53*, 3806−3811.
(12) Irish, D. E.; Jarv, T. *Appl. Spectrosc.* **1983**, *37*, 50−55.
(13) Wahab, A.; Mahiuddin, S. *J. Chem. Eng. Data* **2004**, *49*, 126−132.
(14) Das, B.; Hazra, D. K. *J. Phys. Chem.* **1995**, *99*, 269−273.
(15) Vidulich, G. A.; Evans, D. F.; Kay, R. L. *J. Phys. Chem.* **1967**, *71*, 656−662.
(16) Hinton, J. F.; Amis, E. S. *Chem. Rev.* **1971**, *71*, 627−674.
(17) Hribar, B.; Southall, N. T.; Vlachy, V.; Dill, K. A. *J. Am. Chem. Soc.* **2002**, *124*, 12302−12311.
(18) Hosono, E.; Fujihara, S.; Kimura, T.; Imai, H. *J. Sol−Gel Sci. Technol.* **2004**, *29*, 71−79.
(19) Jolivet, J. P. *Metal Oxides Chemistry and Synthesis, From Solution to Solid State*; Wiley: New York, 2000.
(20) Livage, J.; Sanchez, C.; Henry, M.; Doeuff, S. *Solid State Ionics* **1989**, *32/33*, 633−638.
(21) Frost, R. L.; James, D. W. *J. Chem. Soc., Faraday Trans. 1* **1982**, *78*, 3263−3279.
(22) Major, S.; Kumar, S.; Bhatnagar, M.; Chopra, K. L. *Appl. Phys. Lett.* **1986**, *49*, 394−396.
(23) Nomura, K.; Ohta, H.; Takagi, A.; Kamiya, T.; Hirano, M.; Hosono, H. *Nature* **2004**, *432*, 488−492.
(24) Kumar, B.; Gong, H.; Akkipeddi, R. *J. Appl. Phys.* **2005**, *98*, 073703.
(25) Ku, C.; Duan, Z.; Reyes, P. I.; Lu, Y.; Xu, Y. *Appl. Phys. Lett.* **2011**, *98*, 123511.
(26) Lee, C.; Cobb, B.; Dodabalapur, A. *Appl. Phys. Lett.* **2010**, *97*, 203505.
(27) Hosono, H.; Nomura, K.; Ogo, Y.; Uruga, T.; Kamiya, T. *J. Non-Cryst. Solids* **2008**, *354*, 2796−2800.
(28) Jeong, S.; Lee, J.; Lee, S. S.; Choi, Y.; Ryu, B. *J. Phys. Chem. C* **2011**, *115*, 11773−11780.

(29) Jun, T.; Jung, Y.; Song, K.; Moon, J. *ACS Appl. Mater. Interfaces* **2011**, *3*, 774−781.
(30) Nicollian, E. H.; Berglund, C. N.; Schmidt, P. F.; Andrews, J. M. *J. Appl. Phys.* **1971**, *42*, 5654−5664.
(31) Jeong, S.; Kim, D.; Lee, S.; Park, B.; Moon, J. *Appl. Phys. Lett.* **2006**, *89*, 092101.
(32) Kagan, C. R.; Andry, P. *Thin-Film Transistors*; Marcel Dekker: New York, 2003.
(33) Marley, N. A.; Gaffney, J. S. *Appl. Spectrosc.* **1990**, *44*, 469−476.
(34) Yoo, Y. B.; Park, J. H.; Lee, S. J.; Song, K. M.; Baik, H. K. *Jpn. J. Appl. Phys.* **2012**, *51*, 040201.